Particle Production in Au+Au Collisions at $\sqrt{s_{NN}}$ = 9.2 GeV

Jiayun Chen[*] **(for STAR Collaboration)**

Institution of Particle Physics, Central China Normal University (HZNU), Wuhan 430079,
P.R.China
Physics Department, Brookhaven National Laboratory, Upton, NY 11973, USA
The Key Laboratory of Quark and Lepton Physics (HZNU), Ministry of Education, Wuhan,
430079, P.R.China
E-mail: chenjy@iopp.ccnu.edu.cn

In this report we present the first test run results from Au+Au collisions at $\sqrt{s_{NN}}$ = 9.2 GeV at RHIC. The large acceptance STAR detector has collected 3k minimum bias collisions during this test run. The azimuthal anisotropy, identified particle spectra, particle ratios and HBT radii are observed to be consistent with the previous measurements from CERN SPS at similar center of mass energies. These results from the lowest collision energy at RHIC demonstrate the STAR detector's readiness to collect high quality data for the proposed Critical Point Search Program which allows us to explore the QCD phase diagram.

---

[*]Speaker.

1. Introduction

In the first decade of STAR running, the evidence about the existence of a strongly coupled Quark Gluon Plasma (sQGP) [1] came in the form of strong suppression of particle production at large p_T [2] and the large amount of elliptic flow [3]. As an important step towards understanding the properties of sQGP and the structure of the QCD phase diagram, a systematic analysis of particle production as a function of collision energy is necessary. Theoretical calculations have indicated that the order of the transition from hadronic matter to the sQGP depends on the baryon chemical potential (μ_B) and temperature (T): at low μ_B and high T, a cross-over transition occurs[4]; at high μ_B and low T, the phase transition is thought to become first order [5]; this first order phase transition "meets" with the smooth cross-over at the critical point[6]. Experimentally we can access this phase diagram and vary these initial conditions by changing the beam energy. Thus a beam energy scan (BES) program will help us to explore the QCD phase diagram and to locate the critical point [7, 8]. As a first step of the BES program, RHIC made a test run for Au+Au collisions at $\sqrt{s_{NN}}$ = 9.2 GeV. The preliminary results from STAR will be reported in this article.

2. Experiment and Analysis

The data presented here are from Au+Au collisions at $\sqrt{s_{NN}}$ = 9.2 GeV, recorded by the STAR experiment at RHIC. The main detector used to obtain the results on anisotropy flow, yields, particle ratios and pion interferometry is the Time Projection Chamber (TPC) [9]. The TPC is STAR's primary detector and can track up to 4000 particles per event. For the collisions near its center, the TPC covers the pesudorapidity (η) range $|\eta| \leq 1.5$. The full azimuthal coverage of the TPC makes it ideal for flow and event-by-event fluctuations measurements. The particle identification (PID) is accomplished by measuring the ionization energy loss (dE/dx) in the TPC. In the future, the Time of Flight (ToF) detector [10] (with 2π azimuthal coverage and $|\eta| < 1.0$) will further enhance the PID capability. The ToF will be ready for Run10 in December of 2009.

All events were taken with a minimum bias tigger. The tigger detectors used in this data are the Beam-Beam-Counter (BBC) and Vertex Position Detector (VPD) [11]. The BBCs are scintillator annuli mounted around the beam pipe beyond the east and west pole-tips of the STAR magnet at about 375 cm from the center of the nominal interaction region (IR), and they have the η coverage of $3.8 < |\eta| < 5.2$ and a full azimuthal (2π) coverage. The BBCs are used to reconstruct the first order event plane for the directed flow analysis.

The only result obtained from the forward rapidity windows are the directed flow measurement, for which we used data taken by the Forward Time Projection Chamber (FTPC) [12]. The FTPC detects charged particles in $|\eta|$ range from 2.5 to 4.2 with full azimuthal coverage. The detail about the design and the other characteristics of the STAR detector can be found in Ref. [13].

There are $\sim$ 3000 good events collected at about 0.6 Hz in the year 2008. The data taking period lasted less than 5 hours.

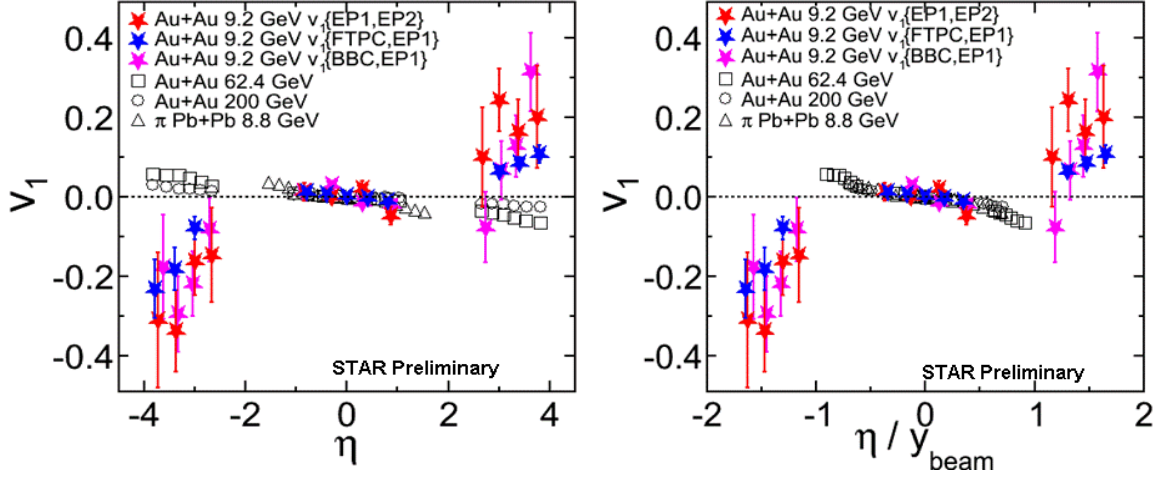The centrality definition and the tracks selection for various analysis are explained in Ref. [14].

Figure 1: Left panel: Charge hadron $v_1 vs. \eta$ from Au+Au collisions at 9.2 GeV in centrality 0-60%. The solid star symbols are the results obtained from the mixed harmonic method (red), the standard methods which include the first order event plane reconstructed by FTPC (blue) and BBC (pink) respectively (see text for details). The results are compared with v_1 from Au+Au collisions at 62.4 GeV (square symbols) and 200 GeV (circle symbols) from centrality 30-60% [16]. The charged pions v_1 from Pb+Pb collisions at 8.8 GeV are also shown [17]. Right panel: Same as the left panel, but plotted as a function of η/y_{beam}. The error bars include only statistical uncertainties.

3. Results and Discussion

Fig. 1 (left panel) shows the charged hadrons v_1 as a function of η in 0-60% most central Au+Au collisions at 9.2 GeV. The p_T range for this study is 0.15-2.0 GeV/c. The v_1 results from 9.2 GeV are obtained by different methods: 1) The standard methods: the one for which the first order event plane is reconstructed from the FTPC tracks is named $v_1\{EP_1, FTPC\}$, while that which uses BBC hits for the first order event plane reconstruction is named $v_1\{EP_1, BBC\}$; 2) The mixed harmonics method, denoted by $v_1\{EP_1, EP_2\}$. This method utilizes the large elliptic flow signal at RHIC, and at the same time suppresses the non-flow arising from the correlation of particles from the same harmonics. The details of these methods can be found in Ref. [15]. The v_1 results at 9.2 GeV from different methods are consistent within the error bars. These results of v_1 from $\sqrt{s_{NN}}$ = 9.2 GeV Au+Au collisions are compared to corresponding results in 30%-60% central Au+Au collisions at 62.4 and 200 GeV [16]. The results are compared with v_1 of charged pions in Pb+Pb collisions at $\sqrt{s_{NN}}$ = 8.8 GeV. At and near mid-rapidity, the v_1 values are independendent of beam energy. At forward rapidities, the v_1 values seem to change sign at lower colliding energy while those at higher energies retain the monotonic behaviour. However, if v_1 are plotted as a function of η scaled with the beam rapidity y_{beam}, as shown in the right plot of Fig. 1, in the common region of values of η/y_{beam} the v_1 values remain the same at all energies.

The elliptic flow versus transverse momentum for the charged hadrons, pions and protons from the 9.2 GeV Au+Au collisions are shown in Fig. 2 (left panel). The comparison with the similar energy from NA49 [17] are also shown. The STAR and NA49 (at $\sqrt{s_{NN}}$ = 8.8 GeV) results seem to be consistent within errors. Fig. 2 (right panel) shows intergral v_2 as a function of beam energy for charged hadrons. Results from minimum bias collisions at 9.2 GeV at midrapidity are compared
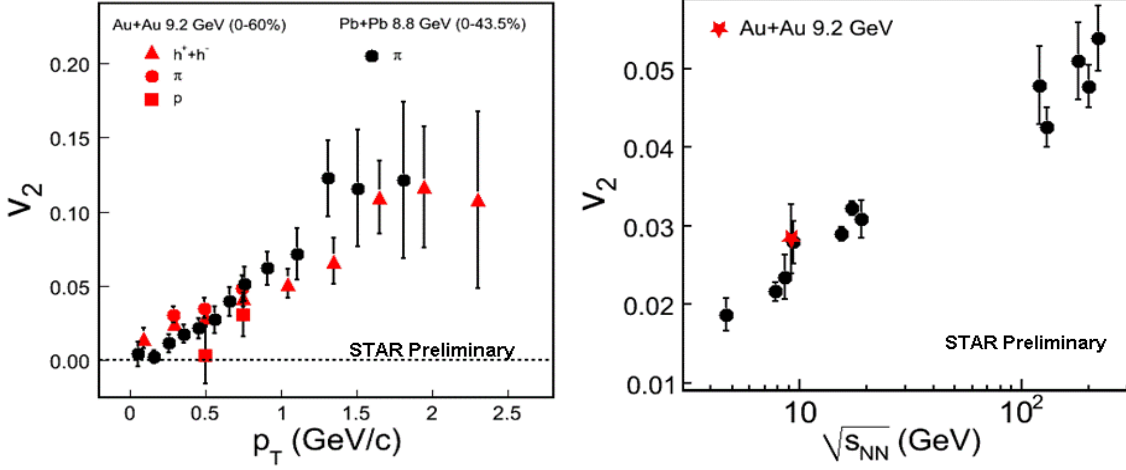
Figure 2: Left panel: v_2 as function of p_T for charged hadrons (red triangles), pions (red circles) and protons (red squares) in 0-60% Au+Au collisions at 9.2 GeV. For comparison, $v_2(p_T)$ results for pions(black circles) from NA49 [17] in 0-43.5% Pb+Pb collisions at 8.8 GeV are shown. Right panel: Energy dependence of integral v_2 ($|\eta| < 1.0$) for Au+Au collisions at 9.2 GeV from centrality 0-60%. The STAR charged hadron v_2 [18] results are compared with the measurement from E877 [19], NA49 [17], PHENIX [20], and PHOBOS [21, 22, 23]. Only statistical error is shown.

with those from STAR at higher energy [18] and other experiments [17, 19, 20, 21, 22, 23]. The v_2 results nicely fits into the observed trends.

Fig. 3 (upper panels) shows the particle yields per unit rapidity dN/dy from $\pi^{\pm}$ and $K^{\pm}$ as a function of $\sqrt{s_{NN}}$ at midrapidity for central collisions. Fig 3 (lower panels) shows the $\langle m_T \rangle - m_0$ for $\pi^{\pm}$ and $K^{\pm}$ respectively in 0-10% central Au+Au collisions at 9.2 GeV. These results are compared to those at AGS, SPS and RHIC energies [24, 25, 26]. The yield and $\langle m_T \rangle - m_0$ beam energy dependence from 9.2 GeV are consistent with the published data. The $\langle m_T \rangle - m_0$ seems to increase with the energy at the AGS energy region $\sqrt{s_{NN}} \sim$ 2-5 GeV. It appears to be independent of the energy in the SPS energy window, $\sqrt{s_{NN}} \sim$ 5-20 GeV. As shown in the figure, the RHIC 9.2 GeV collision data is similar to other results. Assuming a thermodynamic system, the $\langle m_T \rangle - m_0$ is associated with temperature and the $dN/dy \propto \log(\sqrt{s_{NN}})$ represents the entropy of the system. It has been argued that the observations in this scenario could reflect the characteristic signature of a first order phase transition [27]. The energy independence of $\langle m_T \rangle - m_0$, $\sqrt{s_{NN}} \sim$ 8-60 GeV, can be interpreted as reflecting of a mixed phase.

Fig. 4 shows the centrality dependence of particle ratios($K^-/K^+, K^-/\pi^-, p/\pi^+$ and K^+/π^+) from 9.2 GeV (red star symbols) compared with STAR results at high energies 62.4 GeV (open square symbols) and 200 GeV (full circle symbols) [26, 28]. The K^-/K^+ and K^-/π^- ratios are lower in 9.2 GeV compared to that in 200 and 62.4 GeV. On the other hand, There is less variation between 9.2 GeV and the highest RHIC energies in the K^+/π^+ ratio than in case of the other particle ratios just discussed. This reflects that the production of kaons at the mid-rapidity going from a region of high net-baryon density at lower collision energies, to a region of lower net-baryon density at high beam energies. K^+ production at lower beam energies is dominated by associated production. The p/π^+ ratio in 9.2 GeV is greater compared to that in 200 GeV and 62.4 GeV,
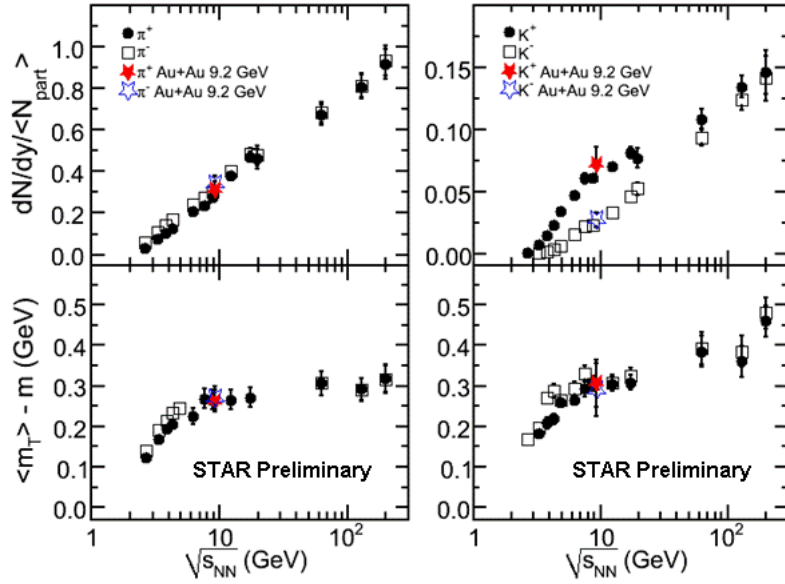
Figure 3: dN/dy normalized by $\langle N_{part} \rangle$ (upper panels) and $\langle m_T \rangle - m$ (lower panels) of $\pi^{\pm}$ (left panels) and $K^{\pm}$ (right panels) in 0-10% central Au+Au collisions for 9.2 GeV compared to previous results from AGS [24],SPS [25] and RHIC [26]. The errors are statistical and systematic errors added in quadrature.
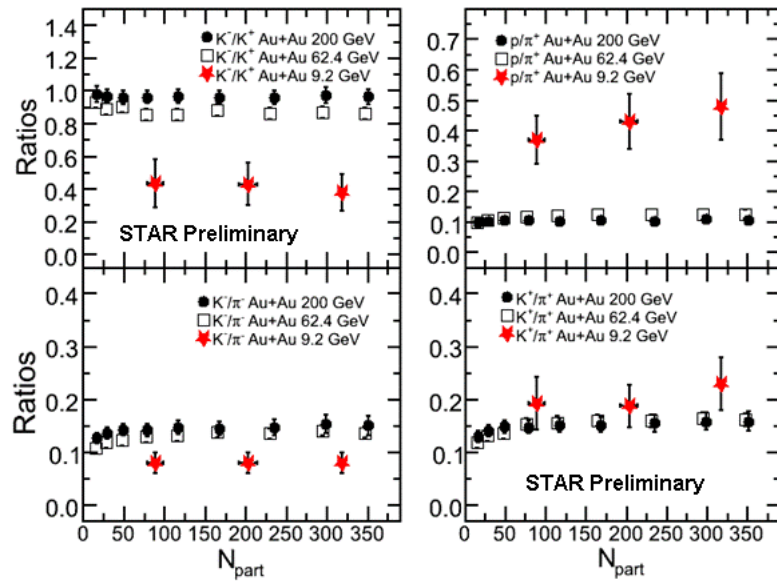

Figure 4: Variation of K^-/K^+ (top left panel), K^-/π^- (bottom left panel), p/π^+ (top right panel) and K^+/π^+ (bottom right panel) from Au+Au collision at 9.2 GeV. The corresponding results from Au+Au collisions at 62.4 GeV and 200 GeV [26, 28] are also shown for comparison. The errors shown are systematic and statistical errors added in quadrature.
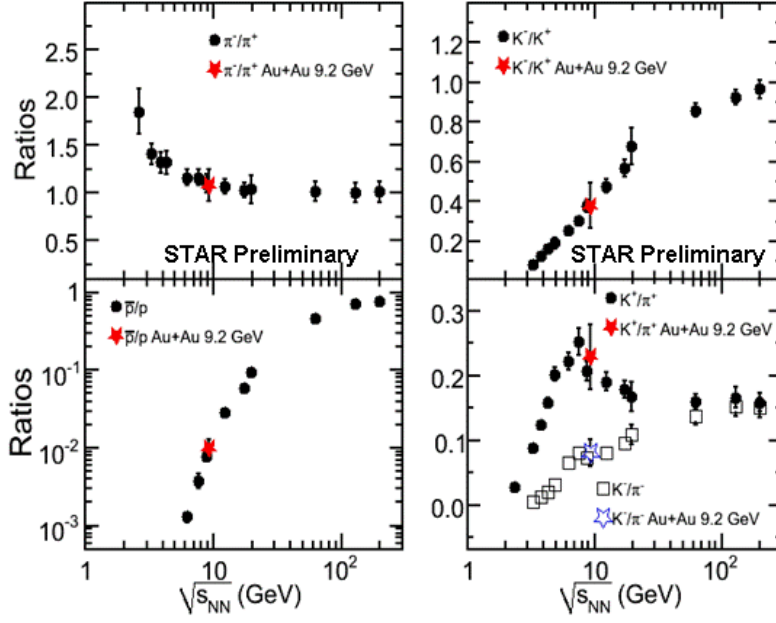
Figure 5: The particle ratios at $|y| < 0.5$ for 0-10% central 9.2 GeV Au+Au collisions are compared to previous results from AGS [24], SPS [25] and RHIC [26] : π^-/π^+(top left panel), $\bar{p}/p$(bottom left panel), K^-/K^+(top right panel) and K/π(bottom right panel). The errors shown are statistical and systematic errors added in quadrature.

reflecting a large baryon stopping at the low energy. All these particle ratios presented seem to be independent of collision centrality for all the energies studied.

Fig. 5 shows the collision energy dependence of particle ratios ($\pi^-/\pi^+, K^-/K^+, \bar{p}/p$ and K/π). The results from Au+Au 9.2 GeV (red star symbol) seem to follow the trends established by the previous measurements [24, 25, 26]. In Au+Au 9.2 GeV collisions, the π^-/π^+ ratio is about 1 which shows that this production is dominated by pair production. The K^-/K^+ ratio is around 0.4, indicating the significant contribution from the associated production for the positive kaons. The $\bar{p}/p$ ratio is far less than one which reflect large baryon stopping. The K/π ratio is of special interest as it expresses the enhancement of strangeness production relative to non-strange hadrons. The K^+/π^+ ratio increases as a function of beam energy and reaches a peak at about $\sqrt{s_{NN}} \sim 7.7$ GeV. At higher beam energies, the ratio starts to show a decreasing trend. The new 9.2 GeV results are found to be consistent with previous observed energy dependence within the error bars. Note that only the ratio of positive particles, K^+/π^+, shows the peak at about 8 GeV. For the negative ratios, a monotonic increase as a function of beam energy is seen, see open-squares in the figure. Since only the K^+ is involved in the associate process ($N+N \rightarrow N+\Lambda+K^+$), the observed peak may reflect the maximum stopping reached in high-energy nuclear collisions. The RHIC BES program will make precision measurements for all of these ratios at this interesting energy region in the near future.

The π interferometry from low p_T and mid-rapidity give us information about the space-time size of emitting source and freeze-out process of the fireball [29]. Fig. 6 shows the results for Hanbury-Brown-Twiss (HBT) pion (π^+) interferometry measurements. There are three
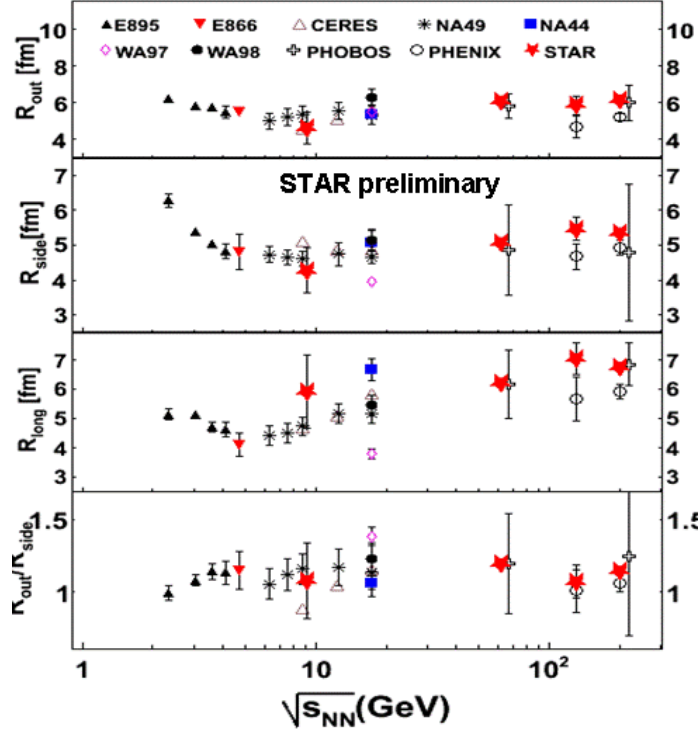
Figure 6: The HBT radii $R_{out}, R_{side}, R_{long}$ and the ratio R_{out}/R_{side} for π^- are plotted as a function of beam energy. The centrality is 0-60% and the k_T range is $[0.15, 0.25]$ (GeV/c) for Au+Au 9.2 GeV. The errors for Au+Au 9.2 GeV are only statistical. The systematic errors are expected to be less than 10% for all radii. The 9.2 GeV results are compared with the measurements by STAR high energies [29], PHENIX [30], PHOBOS [31], NA44 [32], NA49 [33], E802 [34], E866 [35], E895 [36], WA97 [37], CERES [38].

radii parameters R_{out}, R_{side} and R_{long} measured in our analysis. The R_{out} measures the spatial and temporal extension of the source whereas the R_{side} gives the spatial extension of the source. Thus the ratio R_{out}/R_{side} reflects the emission duration of the source. It is expected that the ratio R_{out}/R_{side} is much larger than 1 for a first order transition [39]. For the measured beam energies [29, 30, 31, 32, 33, 34, 35, 36, 37, 38], the ratio R_{out}/R_{side} is close to 1 within errors.

4. Summary and Outlook

In summary, the azimuthal anisotropy (v_1 and v_2) results from Au+Au 9.2 GeV are similar to those obtained from collisions at similar energies. The identified particle spectra are obtained from Au+Au collisions at 9.2 GeV. The centrality and beam energy dependence of the hadron yields and ratios are studied. In the central collisions, the anti-proton to proton ratio ~ 0.01 shows significant baryon stopping in these collisions. The K^-/K^+ ratio from the central collision is ~ 0.4, showing associated production for K^+. The p/π ratio is higher and K^-/π^- is lower at 9.2 GeV compared to 200 GeV at all collision centralities studied. The pion interferometry results in the Au+Au collisions at 9.2 GeV follow the established beam energy trends.

These 9.2 GeV results from Au+Au collision are the first important step towards the RHIC BES program. There are several key measurements for the program: 1) The PID hadron spectra,

ratios and elliptic flow give the information about the collectivity dynamics; 2) The fluctuations including net-proton kurtosis, K/π ratio, $\langle p_T \rangle, \langle N \rangle$ access the thermodynamics of the system. Our BES program is planned to cover the energy range $\sqrt{s_{NN}} \sim 5 - 39$ GeV. Several Lattice QCD based estimates of the Critical Point [4, 5, 6] are within our BES search area. The results presented in this proceedings from the lowest beam energy collisions at RHIC demonstrate the STAR detector's capability to collect high quality data for the proposed BES Program. Large and uniform acceptance for all beam energies in a collider set-up, excellent particle identification (TPC+TOF) and higher statistics will lead to significant advances in the Critical Point search.

References

[1] J.Adams *et al.*, [STAR Collaboration], Nucl. Phys. A **757** (2005) 102.

[2] J.Adams *et al.*, [STAR Collaboration], Phys. Rev. Lett. **91** (2003) 072304.

[3] K.H.Ackermann *et al.*, [STAR Collaboration], Phys. Rev. Lett. **86** (2001) 402.

[4] F.R. Brown *et al.*, Phys. Rev. Lett. **65** (1990) 2491.

[5] O.Scavenius *et al.*, Phys. Rev. C **64** (2001) 045202 ;
N.G.Antoniou *et al.*,Phys. Lett. B **563** (2003) 165 ;
M.Asakawa and K.Yazaki, Nucl. Phys. A **504** (1989) 668 ;
A.Barducci *et al.*, Phys. Lett. B **231** (1989) 463 ;
A.Barducci *et al.*, Phys. Rev. D **41** (1990) 1610;
A.Barducci *et al.*, Phys. Rev. D **49** (1994) 426;
J.Berges and K.Rajagopal, Nucl. Phys. B **538** (1999) 215;
M.A.Halasz *et al.*, Phys. Rev. D **58** (1998) 096007;
Y.Hatta and T.Ikeda, Phys. Rev. D **67** (2003) 014028.

[6] M.A.Stephanov, Prog. Theor. Phys. Suppl. **153** (2004) 139;
M.A.Stephanov, Int. J. Mod. Phys. A **20** (2005) 4387.

[7] Helen Caines (for the STAR Collaboration), Proceedings for *the Rencontres de Moriond 2009 QCD session*, [arXiv:0906.0305v1].

[8] B.I.Abelev *et al.*, [STAR Collaboration] SN0493 : Experimental Study of the QCD Phase Diagram & Search for the Critical Point: Selected Arguments for the Run-10 Beam Energy Scan, http://drupal.star.bnl.gov/STAR/starnotes/public/sn0493.

[9] K.H.Ackermann *et al.*, [STAR Collaboration], Nucl. Instr. Meth. A **499** (2003) 624.

[10] F.Geurt *et al.*, Nucl. Instr. Meth. A **533** (2004) 60;
W.J.Llope, Nucl. Instr. Meth. B **241** (2005) 306.

[11] W.J.Lope *et al.*, Nucl. Instr. Method. A **522** (2004) 252.

[12] K.H.Ackermann *et al.*, [STAR Collaboration], Nucl. Instr. Meth. A **499** (2003) 713.

[13] K.H.Ackermann *et al.*, [STAR Collaboration], Nucl. Instr. Meth. A **499** (2003) 624.

[14] L.Kumar (for the STAR Collaboration), J. Phys. G: Nucl. Part. Phys. **36** (2009) 064066;
D.Das (for the STAR Collaboration), Proceedings for *the 25th Winter Workshop on Nuclear Dynamics*, [arXiv:0906.0630v1].

[15] J.Adams *et al.*, [STAR Collaboration], Phys. Rev. C **72** (2005) 014904

[16] B.I.Abelev *et al.*, [STAR Collaboration], Phys. Rev. Lett. **101** (2008) 252301.

[17] C.Alt *et al.*, [NA49 Collaboration], Phys. Rev. C **68** (2003) 034903.

[18] B.I.Abelev *et al.*, [STAR Collaboration], Phys. Rev. C **75** (2007) 054906.

[19] J.Barrette *et al.*, [E877 Collaboration], Phys. Rev. C **55** (1997) 1420.

[20] A.Adare *et al.*, [PHENIX Collaboration], Phys. Rev. Lett. **98** (2007) 162301.

[21] B.B.Back *et al.*, [PHOBOS Collaboration], Phys. Rev. C **72** (2005) 051901.

[22] B.B.Back *et al.*, [PHOBOS Collaboration], Phys. Rev. Lett. **89** (2002) 222301.

[23] B.Alver *et al.*, [PHOBOS Collaboration], Phys. Rev. Lett. **98** (2007) 242302.

[24] L.Ahle *et al.*, [E866 Collaboration and E917 Collaborartion], Phys. Lett. B **490** (2000) 53;
L.Ahle *et al.*, [E866 Collaboration and E917 Collaborartion], Phys. Lett. B **476** (2000) 1;
J.L.Klay *et al.*, [E895 Collaboraiton], Phys. Rev. Lett. **88** (2002) 102301;
J.Barrette *et al.*, [E877 Collaboration], Phys. Rev. C **62** (2000) 024901;
Y.Akiba *et al.*, [E802 Collaboration], Nucl. Phys. A **610** (1996) 139c;
L.Ahle *et al.*, [E802 Collaboration], Phys. Rev. C **60** (1999) 064901;
L.Ahle *et al.*, [E802 Collaboration], Phys. Rev. C **57** (1998) 466.

[25] S.V.Afanasiev *et al.*, [NA49 Collaboration], Phys. Rev. C **66** (2002) 054902;
C.Alt *et al.*, [NA49 Collaboration], Phys. Rev. C **77** (2008) 024903;
C.Alt *et al.*, [NA49 Collaboration], Phys. Rev. C **73** (2006) 044910;
T.Anticic *et al.* [NA49 Collaboration], Phys. Rev. C **69** (2004) 024902.

[26] B.I.Abelev *et al.* [STAR Collaboration], Phys. Rev. C **79** (2009) 34909.

[27] L.V.Hovw, Phys. Lett. B **118** (1982) 138;
M.Gazdzicki and M.I.Gorenstein, Acta Phys. Polon. B **30** (1999) 2705.

[28] J.Adams *et al.* [STAR Collaboration], Phys. Rev. Lett. **91** (2003) 072304;
J.Adams *et al.* [STAR Collaboration], Phys. Rev. Lett. **91** (2003) 172302;
B.I.Abelev *et al.* [STAR Collaboration], Phys. Rev. Lett. **97** (2006) 152301;
B.I.Abelev *et al.* [STAR Collaboration], Phys. Lett. B **655** (2007) 104.

[29] J.Adams *et al.* [STAR Collaboration], Phys. Rev. C **71** (2005) 044906;
C.Adler *et al.* [STAR Collaboration], Phys. Rev. Lett **87** (2001) 082301.

[30] K.Adcox *et al.* [PHENIX Collaboration], Phys. Rev. Lett **88** (2002) 192302;
S.S.Adler *et al.* [PHENIX Collaboration], Phys. Rev. Lett **93** (2004) 152302.

[31] B.B.Back *et al.* [PHOBOS Collaboration], Phys. Rev. C **73** (2006) 031901.

[32] I.G.Bearden *et al.* [NA44 Collaboration], Phys. Rev. C **58** (1998) 1656.

[33] C.Alt *et al.* [NA49 Collaboration], Phys. Rev. C **77** (2008) 064908.

[34] L.Ahle *et al.* [E-802 Collaboration], Phys. Rev. C **66** (2002) 054906.

[35] R.Soltz *et al.* [E866 Collaboration], Nucl. Phys. A **611** (1999) 439.

[36] M.A.Lisa *et al.* [E895 Collaboration], Phys. Rev. Lett **84** (2000) 2798.

[37] F.Antinori *et al.* [WA97 Collaboration], J. Phys. G **27** (2001) 2325.

[38] D.Adamova *et al.* [CERES collaboration], Nucl. Phys. A **714** (2003) 124.

[39] D.H.Rischke and M.Gyulassy, Nucl. Phys. A **608** (1996) 479.